Human Factors in Simulation, Software and Systems Engineering, Vol. 220, 2026, 135–144
https://doi.org/10.54941/ahfe1007701

Enhancing the Prediction Accuracy of EKASTOS With Individual Parameter Tuning

Chrysovalanto Messiou, Riender Happee, and Georgios Papaioannou

Cognitive Robotics, Delft University of Technology, 2628 CD, Delft, The Netherlands

ABSTRACT

Whole-body vibration strongly influences perceived ride comfort, particularly in automated vehicles, where limited visual cues and unpredictable movements introduce a "surprise factor" that challenges postural stabilization. Conventional seat-to-head transmissibility assessments rely on simplified, linear assumptions that insufficiently represent multi-axis biomechanical responses and neglect inter-individual variability. More detailed and individualized modelling approaches are therefore required. This study, employs Ekastos, a computationally efficient 3D full-body dynamic model developed in Simscape MATLAB, to evaluate its ability to reproduce experimental anterior-posterior whole-body vibration responses across three distinct anthropometries with regards to body size. A hierarchical multi-objective evolutionary optimization framework is implemented to identify model postural control parameters and benchmarked against a gradient-based method. Average (response and anthropometry) seat-to-head frequency-response functions are first compared between experimental data and model responses obtained using the two optimization methods. Model performance is assessed using metrics for head, trunk, and pelvis motion in both X-translation and pitch, comparing model responses against (i) average and (ii) across minimum-maximum range of individual experimental responses. Afterwards, individualization is examined for two subjects by comparing (a) average-optimized postural control parameters with individualized anthropometry and (b) subject-specific postural control parameters with individualized anthropometry. Under average-response conditions, the multi-objective approach reduced objective metrics by 9-31%. Applying average anthropometry and parameters to individuals increased errors by in some cases by more than 100%, whereas anthropometry adaptation and subject-specific tuning reduced errors by up to 47%. These results highlight the necessity of robust optimization and individualization for accurate prediction of seated human dynamic responses under whole-body vibration.

Keywords: EKASTOS, Computational human body model, Anthropometry, Individualization, Whole-body vibration, Postural control

INTRODUCTION

Human exposure to whole-body vibration (WBV) in seated environments remains a central challenge in vehicle design, with direct implications for comfort, postural stability, and musculoskeletal loading (Griffin, 1990; Paddan et al., 2002). These issues are further exacerbated in automated vehicles (AVs),

Received February 20, 2026; Revised April 7, 2026; Accepted April 22, 2026; Available online July 20, 2026

where reduced anticipatory cues and unconventional seating postures increase postural instability and discomfort (Yunus et al., 2025; Papaioannou et al., 2025). Hence, reliable predictive tools are therefore essential for assessing seated human response under vibration. Papaioannou et al., 2025 illustrated this need also for rail and other road vehicles including vicycles.

Seated human response has traditionally been characterized using frequency-response functions (FRFs), such as seat-to-head or seat-to-trunk transmissibility, derived from population-based experiments (Nawayseh et al., 2015; Mirakhorlo et al., 2022). Nevertheless, individual anthropometric and neuromuscular characteristics are known to significantly influence these responses. Paddan et al. (1998,1994) were the first to mention the significant inter-subject variability of their data. Later, Dewangan et al. (2013) explored the effects of gender and anthropometry on the vertical and fore-aft seat-to-head transmissibility response, illustrating that responses were distinctly different between genders. In the same direction, Cvetkovic et al. (2023) proved that by considering motion direction and body segment information, over 72% of the peak translational gains could be explained. Despite these attempts, there is a significant gap in the literature on adaptive seat-to-head transmissibility FRFs or human body models that can capture individual characteristics such as body mass and proportions.

Computational human body models provide an alternative by enabling time-domain simulation of human motion, allowing responses to be evaluated in both the frequency and time domain, which is essential for capturing nonlinear WBV behavior during transient manoeuvres. High-fidelity models, such as the MADYMO Active Human Model (AHM) (Mirakhorlo et al., 2022), have demonstrated strong predictive accuracy under vibration and impact loading, but their computational expense limits their suitability for long-duration comfort studies and large-scale parameter exploration. More lightweight multibody formulations, including scan-based (Pascoletti et al., 2023) and GEBOD-derived models offer improved efficiency but typically lack individualized anthropometry or active postural stabilization. The Efficient Human Model (EHM) (Desai et al., 2024) introduced active control within a simplified geometric framework, with its parameters being calibrated to average experimental responses.

The reliability of such average-based tuning for predicting individual behaviour remains largely unexplored. Moreover, individual-specific calibration is rarely attempted due to computational and optimization challenges. To address these limitations, Messiou et al., (2025) introduced EKASTOS, a full body seated human model with adaptive anthropometry implemented in the Simscape MATLAB environment. EKASTOS integrates multibody dynamics and control within a computationally efficient framework, enabling faster simulations and a more accessible workflow. However, its initial calibration relied on a gradient-based optimization strategy originally developed for EHM, which is susceptible to local minima and sensitive to initialization (Messiou et al., 2025).

In the present study, we extend EKASTOS by adapting the optimization framework to improve robustness and solution-space exploration. A new

multi-objective evolutionary optimization method is introduced and compared against the previous gradient-based method. First, the two optimization methods are evaluated for the average anthropometry and average experimental FRFs to assess improvements in fitting robustness and accuracy. Subsequently, EKASTOS is evaluated across three distinct anthropometries under anterior-posterior excitation. We first investigate the effect of applying a single parameter set optimized for the average response to different anthropometries. We then assess the improvement achieved when postural control parameters are optimized individually for each subject. This study therefore contributes both methodologically and biomechanically: it demonstrates the impact of optimization strategy on model calibration and provides new insight into the relative roles of anthropometry and postural control in human–seat interaction and comfort modelling.

The paper is structured as follows. The experimental data and the revised optimization framework are first described, followed by the presentation of results for average and individualized calibration. Conclusions are then drawn.

METHODS

Experimental Data

WBV data were taken from Mirakhorlo et al. (2022), who conducted experiments on 18 seated subjects subjected to broadband translational excitation in the 0.3–12 Hz frequency range. The input was selected to excite the dominant dynamics relevant to comfort and motion sickness. Experimental responses were quantified using FRFs between the seat and multiple body segments (head, trunk, and pelvis). Subject-specific anthropometric measurements, including linear dimensions, age, and body mass, were collected. The demographic characteristics of the analyzed subjects are summarized as follows: mean age 47 years (SD 13), 5 males and 4 females, mean body mass 77.4 kg (SD 13.6), and mean height 179.1 cm (SD 12.3). From this dataset, the average response and two subjects' responses (with contrasting anthropometries in terms of body size) were selected. The two subjects will be referred to as Individual 1 (m = 59 kg, h = 1.71 m, sex = female) and Individual 2 (m = 100 kg, h = 1.94 m, sex = male) (Figure 1).

Optimization Method for Parameter Identification

Algorithm & Method: To identify the optimal postural control parameters of EKASTOS based on the experimental responses, we follow established practices in modular system identification (Ljung, 1999; Pintelon et al., 2012) and define three sequential optimization stages:

- **Trunk-Head**: Parameters affecting the trunk-to-head transfer functions are optimized first. Due to the terminal nature of the head in the biomechanical chain, these FRFs are independent of pelvis and seat parameters under the LTI assumption *[45 variables total]*.

- **Pelvis-Trunk**: With the head–trunk parameters fixed at their optimal values, parameters governing trunk–pelvis dynamics are identified. At this stage, downstream seat dynamics do not influence the trunk–pelvis transfer functions *[17 variables total]*.
- **Seat-Pelvis**: Finally, parameters governing lower-body and seat interaction are optimized, while all upstream parameters remain fixed *[17 variables total]*.

This optimization methods will be referred as Optimization 2 (new multi-objective framework) and Optimization 1 (gradient-based) will be our reference method as used by Desai et al. (2024). The optimization algorithm adopted for tuning the postural is NSGA-II as it performs well for a limited number of objectives. Specifically, MATLAB *gamultiobj* algorithm was used with the following configurations: PopulationSize = 200, MaxGenerations = 200, vectorized evaluation, and informed initial population.

Objective function (J): As objective for optimally tuning the parameters, we adopt a complex-valued, frequency-domain cost function grounded in classical system-identification principles. Complex residuals provide balanced weighting across frequencies and avoid numerical issues associated with separating magnitude and phase (Ljung, 1999; Pintelon et al., 2012). The evaluation of the objective function is as follows (a) Retain the FRFs (Table 1) as complex quantities, (b) Compute the complex logarithmic ratio error, (c) Weight the error using experimental coherence, (d) Restrict the analysis to the frequency band of interest, (e) Integrate the weighted squared error over frequency. For every optimization stage, two objective functions (J_θ and J_x) are calculated by applying the above procedure separately to the two FRFs considered at that stage (Table 1). Specifically, J_x quantifies the coherence-weighted complex gain error between model and experimental FRFs for the X-translational output response, while J_θ quantifies the corresponding error for the pitch-rotational output response.

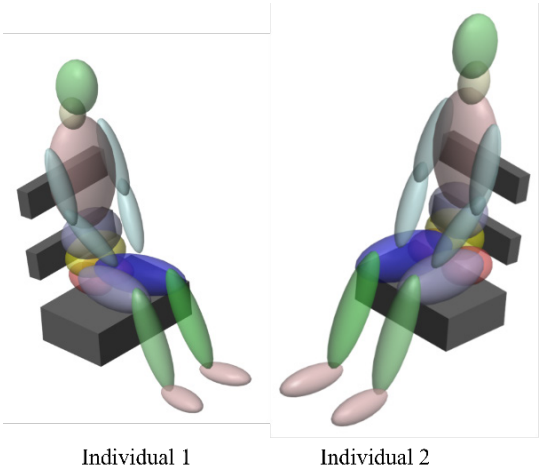

Figure 1: EKASTOS in the body size of Individual 1 (m = 59 kg, h = 1.71 m, sex = female) and Individual 2 (m = 100 kg, h = 1.94 m, sex = male).

Table 1: FRFs used in each optimization stage to calculate the objective function (J).

Optimization Stage	FRFs (Output/ Input)
Trunk-Head	Head X position / Trunk X position
	Head pitch rotation / Trunk X position
Pelvis-Trunk	Trunk X position / Pelvis X position
	Trunk pitch rotation / Pelvis X position
Seat-Pelvis	Pelvis X position / Seat X position
	Pelvis pitch rotation / Seat X position

RESULTS

In this section, we first present the Pareto Fronts (Figure 2) for each optimization stage to demonstrate convergence of the presented optimization method. Next, we compare the average (response and anthropometry) seat-to-head FRFs between the experimental data and model responses. The model responses are obtained using the optimal postural control parameters from Optimization 1 (the gradient-based method by (Desai et al., 2025)) and Optimization 2 (new multi-objective genetic algorithm framework) (Figure 3). The responses are evaluated using J_θ and J_x for every optimization stage (a) between model and experimental FRFs for the average response (Table 2) and (b) between the model and the minimum and maximum individual FRFs (Table 3). Finally, individual seat-to-head FRFs from (a) average-optimized postural control parameters with individualized anthropometry, (b) subject-specific postural control parameters with individualized anthropometry and (c) experimental data are compared for two subjects (Figure 4 and Table 4).

Optimization Efficiency for the Average

The hierarchical, multi-objective optimization converged to well-defined Pareto fronts for each subsystem with limited scatter (Figure 2), indicating robust convergence of the proposed optimization method (Optimization 2). This illustrates that the selected configuration of our algorithm was appropriate to ensure convergence close to the optimum Pareto set. For all the optimization stages, the trade-offs between X-translational (J_x) and pitch-rotational (J_θ) objective functions (Figure 2) were clearly captured in the tuning objectives. The improvement of the fit towards the X-translational response, deteriorates the fit of the pitch-rotational response. This trade-off represents an inherent challenge in parameter identification for coupled biomechanical control systems as also reported by Messiou et al., (2025).

Due to this conflicting nature, a single solution was selected among the optimal set of solutions in the Pareto fronts in post-processing to minimize the compromise between the two objectives for each subsystem (i.e., optimization stage). The single solution is in the middle of the Pareto fronts. Using the average anthropometry and average experimental FRFs, model responses were evaluated with optimal postural control parameters derived from Optimization

Method 1 and 2. For each FRF per optimization stage, Table 2 presents the corresponding gain metrics J computed for the average experimental response. This metric provides a direct comparison of fitting performance between Optimization Methods 1 and 2. Across 5/6 FRFs, the Optimization 2 achieved lower J values ~9–31%. Only the last objective function had a marginally higher J value (3.45%) in comparison to Optimization 1. These indicate the improved fitting accuracy under average conditions.

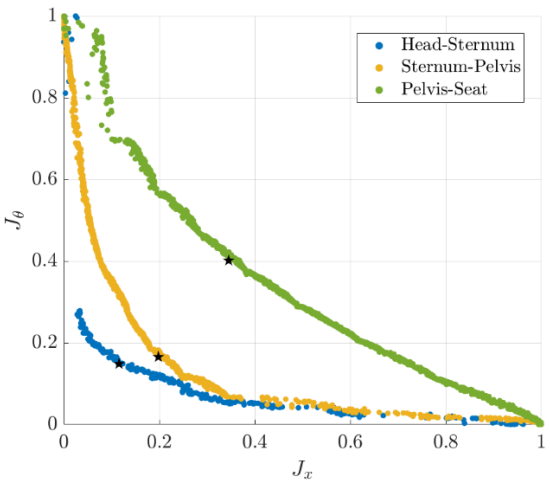

Figure 2: Pareto fronts, from Optimization 2, for head–trunk, trunk–pelvis, and pelvis–seat subsystems (different optimization stages), showing the trade-off between X-translational (J_x) and pitch-rotational (J_θ) objective functions J. The objective functions are normalized. Single solution per optimization stage is denoted as star per Pareto front.

Table 2: Comparison of complex gain metric J for the average experimental FRF versus average model response. For each FRF, model responses are obtained using parameters derived from Optimization 1 and Optimization 2.

Optimization Stage	Objective Function	Optimization 1	Optimization 2
1	J_{x1}	3.22	**2.62**
	$J_{\theta 1}$	4.07	**2.92**
2	J_{x2}	2.05	**1.62**
	$J_{\theta 2}$	3.56	**3.24**
3	J_{x3}	1.30	**0.90**
	$J_{\theta 3}$	**3.48**	3.60

Individual Prediction With Average-Based Parameters and Anthropometry

With regards to the accuracy of the model in individual responses, Table 3 presents the difference in the objective functions between average-based model response and minimum and maximum individual FRFs (as

extracted from the dataset, Figure 3 edges of the shaded area). More specifically, across optimization stages, deterioration of the fit ranges from approximately 1-4% for the least variable FRFs (e.g., trunk and pelvis pitch) to over 100% for the most variable responses (e.g., trunk and pelvis X), while head pitch reached differences of approximately 52%. These differences are also illustrated in Figure 3, which shows the seat-to-head FRFs. The experimental data are plotted with a shaded area representing the range of individual FRFs, while model responses are plotted using the optimal model parameters from the two optimization methods. These results highlight the limitations of average-based tuning and emphasize the necessity of adapting both the model's postural control parameters and anthropometry to the individual. The background shading indicates the experimental coherence used to weight the complex gain metric *J*.

Individual Prediction With Individual Parameters and/or Anthropometry

With the model anthropometry adapted to match each individual subject, the FRFs were evaluated under two conditions: (1) using postural control parameters optimized specifically for the individual, and (2) using the parameters derived from the average-response tuning. Figure 4 show the seat-to-head FRFs for Individual 1 and 2, respectively, alongside the experimental data. Shaded areas indicate the experimental coherence weighting used in the computation of the complex gain metric *J*. Table 4 summarizes the corresponding metric values.

For Individual 1, adapting anthropometry alone already yields a good agreement with the experimental data, both in magnitude and overall shape of the FRFs (Figure 4). Subject-specific tuning of the postural control parameters provides only marginal additional improvement (Table 4). In contrast, for Individual 2, the model response obtained with average-optimized postural control parameters deviates not only in magnitude but also in the overall shape of the FRFs (Figure 4). Subject-specific tuning substantially improves the agreement, reducing *J* by approximately 5–47% across most responses, with the largest improvements observed for head X and pitch responses, which were also identified as sensitive in the population-average analysis. Responses such as pelvis X, although highly variable across the population, show minimal change for Individual 2 once the model anthropometry is adapted. This indicates that individualized postural control tuning has a comparatively smaller influence on these dynamics.

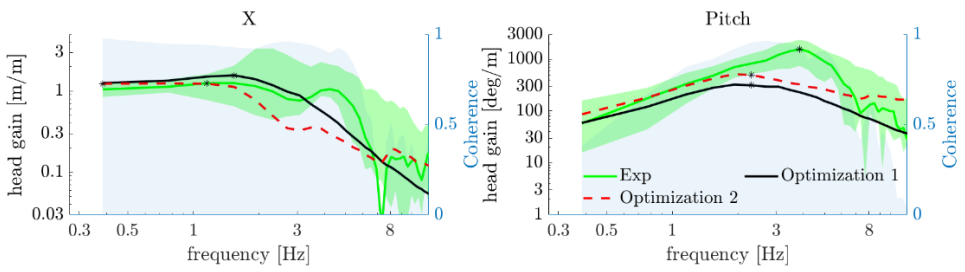

Figure 3: Seat-to-head FRFs for average anthropometry: experimental data (shaded range of individual FRFs) compared with model responses using parameters obtained from Optimization 1 and 2. Background shading shows coherence weighting for J.

Table 3: Comparison of complex gain metric *J* using Optimization 2 (new). For each FRF, values correspond to comparisons between the minimum (MIN) and maximum (MAX) (edges of the shaded areas) individual experimental FRFs and the model response obtained with the average-based parameters.

Optimization Stage	Objective Function	Optimization 2	
		MIN	*MAX*
1	Jx1	1.99	3.97
	Jtheta1	2.89	3.99
2	Jx2	2.17	3.38
	Jtheta2	3.30	4.39
3	Jx3	1.53	1.90
	Jtheta3	3.74	4.49

CONCLUSION

This study introduced a revised multi-objective optimization framework for EKASTOS to robustly identify postural control parameters under seated whole-body vibration and explored EKASTOS's prediction accuracy for individual responses. By replacing gradient-based tuning with a Pareto-based evolutionary approach and implementing a structured hierarchical optimization sequence, the robustness and reliability of parameter identification were significantly improved. The new optimization method achieved consistently lower complex gain metrics J for the average response in 5 out of 6 frequency-response functions (≈9–31% improvement), demonstrating enhanced fitting accuracy under population-average conditions.

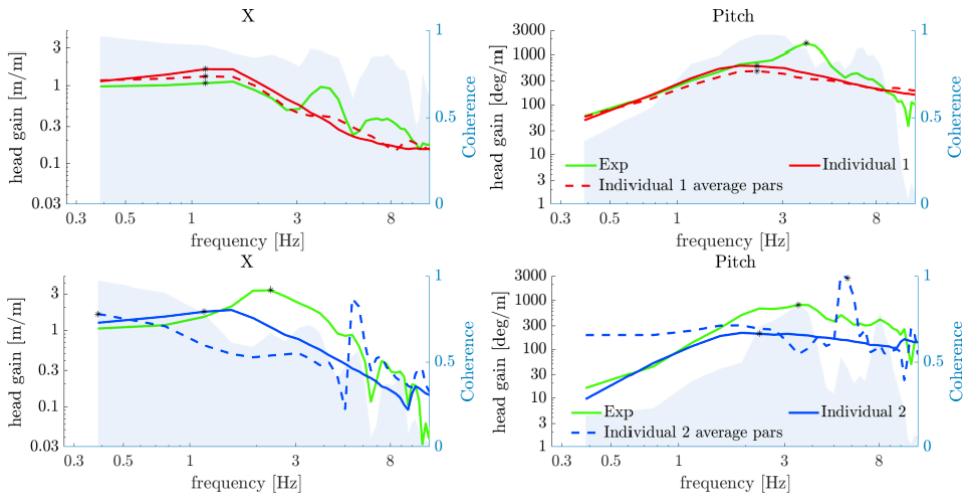

Figure 4: Individual seat-to-head FRFs for Individual 1 (top) and Individual 2 (bottom). Model responses use average-optimized or subject-specific postural control parameters with individualized anthropometry; shading shows experimental coherence.

Table 4: Complex gain metrics *J* for Individual 1 and Individual 2 subjects comparing model responses using average-optimized parameters versus subject-specific optimized parameters.

Optimization Stage	Objective Function	Individual 1		Individual 2	
		Subject	*Average*	*Subject*	*Average*
1	J_{x1}	2.93	**1.81**	**2.06**	3.58
	$J_{\theta 1}$	**2.10**	2.20	**2.42**	4.58
2	J_{x2}	2.40	**2.07**	**2.06**	2.18
	$J_{\theta 2}$	**3.45**	3.75	**2.05**	2.36
3	J_{x3}	1.74	1.74	0.66	**0.62**
	$J_{\theta 3}$	**3.78**	4.08	**2.67**	3.09

Analysis of the minimum–maximum range across individuals revealed substantial deterioration when a single, average-optimized parameter set was applied to represent the full population. Depending on the frequency-response function, deterioration ranged from approximately 1-4% for the least sensitive responses to over 100% for the most sensitive ones, with head pitch responses reaching differences of approximately 52%. These findings highlight the inherent limitations of population-average tuning.

When the model anthropometry was adapted to individual subjects, the effect of subject-specific postural control tuning differed between participants. For Individual 1, anthropometric adaptation alone already provided good agreement with the experimental data, with only marginal additional improvement from subject-specific parameter tuning. In contrast, for Individual 2, subject-specific optimization reduced the objective function by approximately 5–47%, particularly for head and trunk responses, and corrected deviations in the overall shape of the frequency-response functions. The above findings indicate that while anthropometric adaptation can be sufficient for some individuals, others require individualized neuromuscular control tuning to accurately reproduce their dynamic behaviour.

Overall, the results confirm two key points:

1. Robust multi-objective optimization improves confidence in parameter identification under average conditions.
2. Individualized tuning is essential to capture the full range of seated human dynamic responses under WBV, especially for responses that are highly sensitive to anthropometry and postural control.

ACKNOWLEDGMENT

The authors would like to acknowledge the support by MathWorks through the award for EKASTOS project.

REFERENCES

Chaudhari, P., Thakur, A. K., Kumar, R., Banerjee, N., & Kumar, A. (2022). Comparison of NSGA-III with NSGA-II for multi objective optimization of adiabatic styrene reactor. *Materials Today: Proceedings*, 57, 1509–1514.

Cvetkovic, M., Desai, R., Papaioannou, G., & Happee, R. (2023). Kinematic body responses and perceived discomfort in a bumpy ride: Effects of sitting posture. *arXiv preprint arXiv:2310.05923*.

Desai, R., Papaioannou, G., & Happee, R. (2025). Vibration transmission through the seated human body captured with a computationally efficient multibody model. *Multibody System Dynamics*, 65(1), 1–34.

Dewangan, K. N., Shahmir, A., Rakheja, S., & Marcotte, P. (2013). Vertical and fore-aft seat-to-head transmissibility response to vertical whole body vibration: Gender and anthropometric effects. *Journal of Low Frequency Noise, Vibration and Active Control*, 32(1-2), 11–40.

Griffin, M. J. (2012). *Handbook of human vibration*. Academic Press.

Ljung, L. (1999). *System identification: Theory for the user*. Prentice Hall.

Messiou, C., Happee, R., & Papaioannou, G. (2025). EKASTOS: Individualized human body model for seated occupants in automated vehicles. *Preprint*.

Messiou, C., Happee, R. and Papaioannou, G. (2025) 'MPC-based postural control: Mimicking CNS strategies for head–neck stabilization under eyes closed conditions', *Control Engineering Practice*, 164, 106428. doi:10.1016/j.conengprac.2025.106428.

Mirakhorlo, M., Kluft, N., Desai, R., Cvetković, M., Irmak, T., Shyrokau, B., & Happee, R. (2022). Simulating 3d human postural stabilization in vibration and dynamic driving. *Applied Sciences*, 12(13), 6657.

Mirakhorlo, M., Kluft, N., Shyrokau, B., & Happee, R. (2022). Effects of seat back height and posture on 3D vibration transmission to pelvis, trunk and head. *International Journal of Industrial Ergonomics*, 91, 103327.

Nawayseh, N. (2015). Effect of the seating condition on the transmission of vibration through the seat pan and backrest. *International Journal of Industrial Ergonomics*, 45, 82–90.

Paddan, G. S., & Griffin, M. J. (1988). The transmission of translational seat vibration to the head—II. Horizontal seat vibration. *Journal of Biomechanics*, 21(3), 199–206.

Paddan, G. S., & Griffin, M. J. (1994). Transmission of roll and pitch seat vibration to the head. *Ergonomics*, 37(9), 1513–1531.

Paddan, G. S., & Griffin, M. J. (2002). Effect of seating on exposures to whole-body vibration in vehicles. *Journal of Sound and Vibration*, 253(1), 215–241.

Papaioannou, G., Shen, C., Rothhämel, M., & Happee, R. (2025). Occupants' comfort: What about human body dynamics in road and rail vehicles? *Vehicle System Dynamics*, 63(7), 1241–1299.

Pascoletti, G., Huysmans, T., Molenbroek, J. F. M., & Zanetti, E. M. (2024). From an ellipsoid-based to an anthropomorphic articulated total body model for multibody applications. *International Journal on Interactive Design and Manufacturing (IJIDeM)*, 18(8), 5991–6011.

Pintelon, R., & Schoukens, J. (2012). *System identification: A frequency domain approach*. John Wiley & Sons.

van der Kruk, E. (2025). BIASMECHANICS: Does an unconscious bias still persist in biomechanics, positioning males as the default in human research? A meta-analysis on the Journal of Biomechanics 2024 publications. *Journal of Biomechanics*, 181, 112560.

Yunus, I., Papaioannou, G., Jerrelind, J., & Drugge, L. (2024). A review of vehicle dynamics and control-based approaches for mitigating motion sickness in autonomous vehicles.